Cu–Co bimetallic nanospheres embedded in graphene as excellent anode catalysts for electrocatalytic oxygen evolution reaction

Wei Sun[1], Fan Fei[2], Jianbo Zheng[1], Guanghua Mao[2], Wei Wei[1] ✉, Jimin Xie[1]

[1]*School of Chemistry and Chemical Engineering, Center of Analysis and Test, Jiangsu University, Zhenjiang 212013, People's Republic of China*
[2]*School of the Environment and Safety Engineering, Jiangsu University, Zhenjiang 212013, People's Republic of China*
✉ *E-mail: weiwei@ujs.edu.cn*

Published in Micro & Nano Letters; Received on 26th October 2018; Accepted on 3rd January 2019

In this work, novel Cu–Co bimetal/reduce graphene oxide nanostructures with excellent catalytic activity were prepared by embedding Cu–Co bimetallic nanospheres into the interlayer of graphene. The composite materials were characterised by X-ray diffraction (XRD), Fourier transform infrared (FTIR), and scanning electron microscopy (SEM) etc. The characterisation results indicated that the diameters of the bimetallic nanospheres were controlled within ~60 nm, which embedded uniformly in graphene. A series of electrochemical tests were carried out and the composites were found to exhibit excellent oxygen evolution properties under alkaline conditions. The excellent catalytic activity and stability make the composite have great potential for wide application and provide a basis for its industrial application.

1. Introduction: In the face of the dual pressures of environment and energy, hydrogen energy was widely recognised as a new type of green energy that can replace fossil energy. Among the many hydrogen production methods, electrolysed water hydrogen production technology was considered to be the most probable large-scale hydrogen production technology, but higher energy consumption restricted its development [1, 2]. An excellent anode oxygen evolution catalyst can reduce the oxygen evolution overpotential and thus reduces the energy consumption. In recent years, a large number of anode catalyst materials have been developed [3]. Among them, noble metals have excellent performance. For example, noble metals such as Pt, Ru, Ir, and Pd have excellent oxygen evolution catalytic activity in alkaline solution, and their corresponding oxides also have higher oxygen evolution activity [4]. However, whether simple metals or oxide thereof, the anodic polarisation phenomenon was severe under strong alkaline conditions, which may cause the electrode to be rotted, thereby causing a decrease in oxygen evolution activity. In addition, the relatively small stock of raw materials also limits the application of precious metal materials. Therefore, the development of some other transition metals in place of precious metals has attracted great interest. Non-precious metal materials such as Ni, Co, Zr etc. have been extensively studied because of their oxygen evolution activity close to noble metals [5, 6]. Compared to single metal oxygen evolution catalysts, bimetallic catalysts are composed of two different metals and have superior catalytic activity and catalytic efficiency because bimetallic catalysts not only inherited the intrinsic catalytic properties of each component but also had a strong synergy between metals [7]. Alloys such as Ni–Co [8] and Ni–Fe [9] have been reported to have a lower oxygen evolution overpotential. Kibria and Tarafdar found that the presence of Cu in the alloy can greatly increase the activity of the Ni electrode and reduce the oxygen evolution overpotential after a series of scientific studies [10]. In addition, if a magnetic metal is present in the alloy, the catalyst can be easily recovered by magnetic separation to be reused [11]. Co and Cu were selected as the target materials because the high-catalytic activity of Co and the high conductivity of Cu can complement defects of each other and enhance the catalytic activity by synergistic action [12].

In order to improve the stability of the transition metal catalyst in the redox process, the catalyst carrier strategy has been extensively explored [13]. Compared with other carbon materials, graphene has received extensive attention due to its large specific surface area, excellent electrical conductivity and thermal stability, high-thermal conductivity and remarkable mechanical strength [14]. In addition, it exhibits fascinating electrochemical properties including wide electrochemical potential windows, excellent electrochemical activity and low charge transfer resistance [15]. These excellent properties make graphene an excellent catalyst base material. In addition, previous reports indicated that the nanostructure of the electrocatalyst is also critical for catalytic activity [16]. The use of graphene as a carrier greatly reduced the aggregation of metal nanoparticles and enhanced the active site [17]. On the other hand, the presence of metal nanoparticles may hinder the redeposition of the graphene layer and increased the space between the layers which preserved the large specific surface area of graphene [18].

In this work, a novel Cu–Co bimetal/reduced graphene oxide (rGO) nanostructure with excellent catalytic activity was prepared by inserting Cu–Co bimetallic nanospheres into the reduced graphene intermediate layer by one-step hydrothermal method and explored the effect of annealing temperature on the sample. We expect it to have excellent catalytic oxygen evolution activity and stability. The simple and effective preparation of composite materials in this Letter also provided new ideas for the preparation of other bimetallic catalytic materials and provided a basis for its industrial application.

2. Experimental: First, graphene oxide (GO) was prepared by the modified Hummers method [19]. Next, a total of 2 mmol Cu $(CH_3COO)_2$ and 4 mmol $Co(CH_3COO)_2$ were weighed and dissolved in 20 ml deionised water. 7.5 mg/ml of GO dispersion liquid was added into 10 ml solution and stirred until the mixture was evenly dispersed. Then 16 mmol $CO(NH_2)_2$, which was dissolved in 10 ml deionised water, was slowly added to the solution and stirring was continued to 30 min. The mixture was transferred to a stainless steel autoclave with a volume of 50 ml and the autoclave was placed in 150°C for 4 h. Afterwards, the precipitates were washed three times with deionised water and absolute ethanol. Finally, the obtained precursor was dried under vacuum at 60°C overnight and annealed under argon flow at 400, 500 or 600°C for 2 h to obtain Cu–Co/rGO nanomaterials, which marked as

doi: 10.1049/mnl.2018.5659

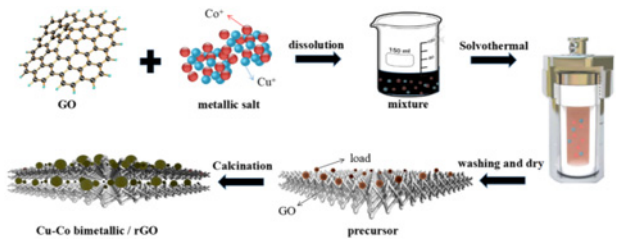

Fig. 1 *Preparation process of Cu–Co bimetal/rGO nanomaterials*

CCG-1, CCG-2, and CCG-3, respectively. The synthesis process is shown in Fig. 1.

Characterisation: The 2θ is in the range of 10–80° using a scanning electron microscope (Bruker D8 Advance) with Cu Kα radiation ($\lambda = 1.5406$ Å) at a scan rate of 7°/min. Scanning electron microscopy (SEM) images were obtained under a JEOL JSM-7001F field emission electron microscope. Test Fourier transform infrared (FTIR) spectroscopy (Nicolet NEXUS 470) collected by KBr pelleting.

Electrocatalytic performance tests: The electrochemical properties of the catalyst electrode were tested by a three-electrode system with the prepared catalyst coated electrode as the working electrode, the saturated calomel electrode as the reference electrode and the platinum electrode as the auxiliary electrode. The test temperature was ambient temperature, and the electrolyte was 1 M KOH solution. The activity of the catalyst was obtained at a scan rate of 0.5 mV/s to obtain an oxygen release reaction (OER) polarisation curve. In addition, the time-current curve is tested to investigate its stability.

3. Results and discussion: The crystalline nature and phase formation of CCG prepared at different temperatures were characterised by X-ray diffraction (XRD) as shown in Fig. 2. Stronger diffraction peaks could be observed as follows: 2θ values 43.297° and 44.216° correspond to the (111) plane, 50.433° and 51.522° correspond to the (200) plane, and 74.130° and 75.853° correspond to the (220) plane. All diffraction peaks were identical to the standard cards for Cu and Co (JCPDS Card No. 04–0836 and JCPDS Card No. 15–0806), which indicated the Cu–Co bimetal was successfully prepared. In addition, a broad diffraction peak appeared at 30° which corresponds to the (002) plane of rGO [20]. Therefore, Cu–Co bimetal/rGO nanomaterials were successfully prepared. It was worth noting that with the annealing temperature increasing, the intensity and sharpness of the diffraction peaks are enhanced, indicating that the crystallinity is improved.

The morphology and size of the as-prepared samples were further investigated by SEM. Figs. 3*a–c* show the microstructure of CCG-1, CCG-2, and CCG-3, respectively. It could be observed that rGO was used as the substrate, and nanometal particles were embedded in the interior and surface of rGO. The obvious difference was that as the temperature of the annealing treatment increases, the distribution and particle size of the nanoparticles became more uniform until 600°C and reaches a uniform nanosphere with a diameter of 60 nm. This was due to the high crystallinity of the product, which was consistent with the results of XRD.

Fig. 4 shows the FTIR spectra of CCG-1, CCG-2, and CCG-3 to further investigate the chemical compositions. There was only a peak at 3500 cm^{-1} compared to GO in the literature [21], and all of the remaining organic functional groups disappear, indicating that GO has been reduced to rGO during this process. In addition, it can be seen that the peak positions and peak numbers of these samples are similar, which indicated that the surface compositions of all the samples were similar, and the smaller difference was due to the influence of the annealing temperature on the purity and the crystal form.

Cyclic voltammetry was used to describe the activity of Cu–Co bimetal/rGO nanomaterials. As shown in Fig. 5*a*, CCG-2 and CCG-3 exhibited greater peak currents at the same voltage to CCG-1, indicating that more active sites were produced which increased the catalytic activity of the OER. The redox peak of CCG-3 was more pronounced than CCG-2 probably due to the more uniform distribution of CCG-3, which is consistent with the results of XRD and SEM. Fig. 5*b* shows the cyclic voltammetry of CCG-3 with different measurement speeds from 2 to 50 mV/s.

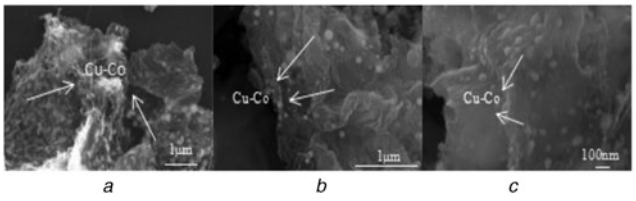

Fig. 3 *SEM images of the as-prepared samples*
a CCG-1
b CCG-2
c CCG-3

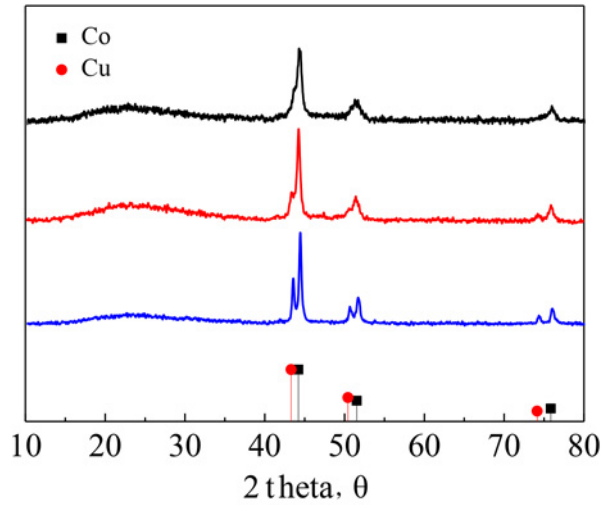

Fig. 2 *XRD patterns of the as-prepared samples*

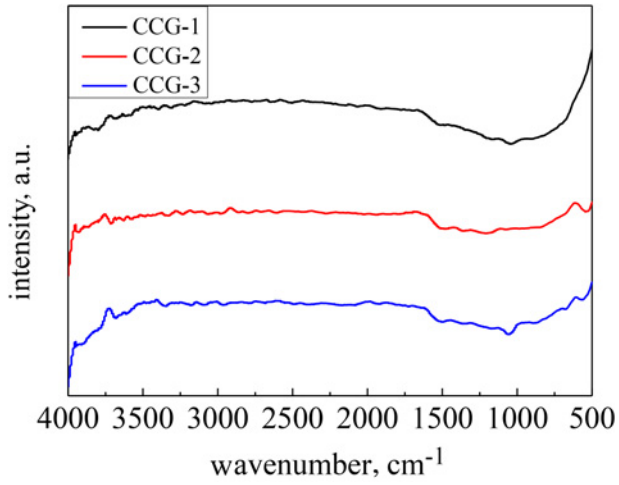

Fig. 4 *FTIR of as-prepared samples*

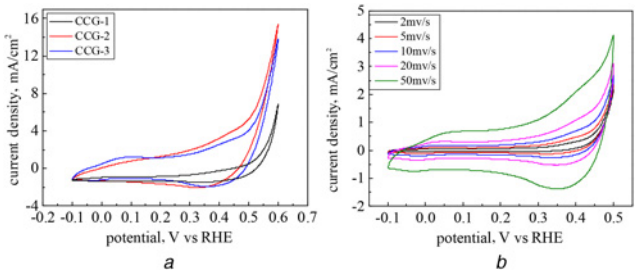

Fig. 5 Cyclic voltammogram
a of as-prepared samples
b of CCG-3 with different measurement speeds

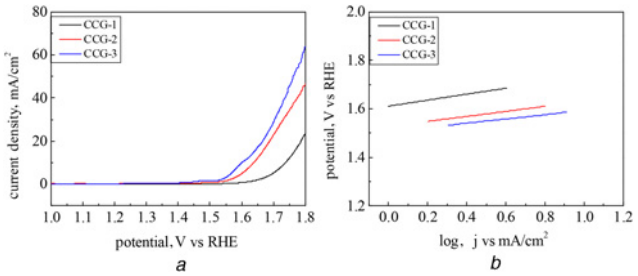

Fig. 6 Electrochemical OER performances of the obtained catalysts
a Polarisation curves of as-prepared samples
b Tafel plot of as-prepared samples

It could be seen from the figure that as the scan rate increases, no significant change in the shape of the curve was observed except for the increase in peak current at the same voltage, which means that CCG-3 had rapid electron transport and high rate capability. In addition, it was also shown that the electrode active material had good reversibility during charging and discharging.

The OER performance of Cu–Co bimetal/rGO nanomaterials was measured using linear sweep voltammetry in 1.0 M KOH solution at a scan rate of 5 mV/s. The polarisation curves are shown in Fig. 6*a* which demonstrated the geometric current density against applied potential after iR correction. It can be seen the onset potentials of CCG-1, CCG-2, and CCG-3 were 1.76, 1.54, and 1.45 V, respectively, which indicated CCG-3 has the best OER activity because of its lowest onset potential. In addition, compared with CCG-1 (490 mV) and CCG-2 (400 mV), CCG-3 had the lowest oxygen evolution overpotential (340 mV) at a current density of 10 mA/cm^2, which indicated that CCG-3 has a good catalytic activity for the OER [22]. This excellent catalytic activity of CCG-3 can be attributed to the uniform embedding of the Co–Cu nanospheres in the graphene intermediate layer to increase the specific surface area and increase the voids, which provided more active sites for electrolyte permeation to improve OER activity. In addition, the superior OER activity of materials was further proved by the Tafel slope as shown in Fig. 6*b*. The Tafel curves were plotted using the equation $\eta = a + b\log(j)$, where η, a, b, and j represent the overpotential, fitting parameter, Tafel slope, and current density, respectively. It could be seen that the lowest Tafel slope of 91.2 mV/dec obtained by the CCG-3 catalyst was smaller than that of CCG-1 (122.7 mV/dec) and CCG-2 (105.4 mV/dec), which further reveals CCG-3 has more favourable reaction kinetics for OER.

As is observed in Fig. 7, the stability of OER was also evaluated by chronoamperometric in 1.0 M KOH at a continuous electrocatalytic voltage of 0.53 V for 8 h, which is due to the stability was a critical parameter for a superior catalyst. CCG-3 maintained a current density >80% after 8 h of energisation compared to CCG-1 and CCG-2 due to the purity and uniform structure of

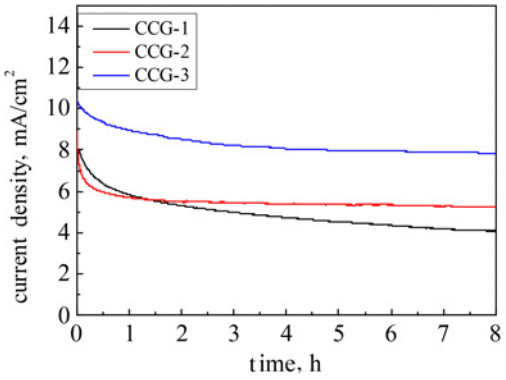

Fig. 7 *Stability of as-prepared samples*

the catalyst. These results suggested the outstanding catalytic performance and great stability of Cu–Co bimetal/rGO nanomaterials, which provided a foundation for industrial applications.

4. Conclusion: A novel Cu–Co bimetal/rGO nanostructure with excellent catalytic activity was prepared by inserting Cu–Co bimetallic nanospheres into the rGO intermediate layer by the one-step hydrothermal method. The process is simple and easy to control. The effects of different annealing temperatures on the morphology and properties of Cu–Co bimetal/rGO nanostructures were investigated. With the increase of calcination temperature, the Cu–Co bimetallic nanospheres are more uniform in size and more evenly distributed in the graphene. The sample at 600°C has the highest catalytic activity compared to others due to the smallest oxygen evolution overpotential. In addition, the current density of 80% or more can be maintained after continuous application of voltage for 8 h, indicating that it also has excellent stability. The excellent catalytic activity and stability make the composite have great potential for wide application and provide a basis for its industrial application.

5. Acknowledgments: This work was supported by the National Natural Science Foundation of China (grant no. 21607063) and the China Postdoctoral Science Foundation (grant no. 2018M630530).

6 References

[1] Zeng M., Li Y.: 'Recent advances in heterogeneous electrocatalysts for the hydrogen evolution reaction', *J. Mater. Chem. A*, 2015, **3**, (29), pp. 14942–14962
[2] Gong M., Dai H.: 'A mini review of NiFe-based materials as highly active oxygen evolution reaction electrocatalysts', *Nano Res.*, 2015, **8**, (1), pp. 23–39
[3] Man I.C., Su H.Y., Calle-Vallejo F., *ET AL.*: 'Universality in oxygen evolution electrocatalysis on oxide surfaces', *ChemCatChem*, 2011, **3**, (7), pp. 1159–1165
[4] Zeng K., Zhang D.: 'Recent progress in alkaline water electrolysis for hydrogen production and application', *Prog. Energy Combust.*, 2010, **36**, (3), pp. 307–326
[5] Stern L.A., Feng L., Song F., *ET AL.*: 'Ni_2P as a Janus catalyst for water splitting: the oxygen evolution activity of Ni_2P nanoparticles', *Energy Environ. Sci.*, 2015, **8**, (8), pp. 2347–2351
[6] Zhao Y., Chen S., Sun B., *ET AL.*: 'Graphene–Co_3O_4 nanocomposite as electrocatalyst with high performance for oxygen evolution reaction', *Sci. Rep.*, 2015, **5**, p. 7629
[7] You B., Jiang N., Sheng M., *ET AL.*: 'Bimeta-organic framework self-adjusted synthesis of support-free nonprecious electrocatalysts for efficient oxygen reduction', *ACS Catal.*, 2015, **5**, (12), pp. 7068–7076
[8] Chi B., Li J., Yang X., *ET AL.*: 'Deposition of Ni–Co by cyclic voltammetry method and its electrocatalytic properties for oxygen evolution reaction', *Int. J. Hydrog. Energy*, 2005, **30**, (1), pp. 29–34
[9] Landon J., Demeter E., Inogglu N., *ET AL.*: 'Spectroscopic characterization of mixed Fe-Ni oxide electrocatalysts for the oxygen

doi: 10.1049/mnl.2018.5659

evolution reaction in alkaline electrolytes', *ACS Catal.*, 2012, **2**, (8), pp. 1793–1801
[10] Kibria A.K.M.F., Tarafdar S.A.: 'Electrochemical studies of a nickel-copper electrode for the oxygen evolution reaction (OER)', *Int. J. Hydrog. Energy*, 2002, **27**, (9), pp. 879–884
[11] Du Y., Cao N., Yang L., *ET AL.*: 'One-step synthesis of magnetically recyclable rGO supported Cu@Co core–shell nanoparticles: highly efficient catalysts for hydrolytic dehydrogenation of ammonia borane and methylamine borane', *New J. Chem.*, 2013, **37**, (10), pp. 3035–3042
[12] Aqueel Ahmed A.T., Hou B., Chavan H. S., *ET AL.*: 'Self-assembled nanostructured $CuCo_2O_4$ for electrochemical energy storage and the oxygen evolution reaction via morphology engineering', *Small*, 2018, **14**, p. 1800742
[13] Niu Q., Guo J., Tang Y., *ET AL.*: 'Sandwich-type bimetal-organic frameworks/graphene oxide derived porous nanosheets doped Fe/Co–N active sites for oxygen reduction reaction', *Electrochim. Acta*, 2017, **255**, pp. 72–82
[14] Novoselov K.S., Fal V.I., Colombo L., *ET AL.*: 'A roadmap for graphene', *Nature*, 2012, **490**, (7419), p. 192
[15] Chen Z., Yu D., Xiong W., *ET AL.*: 'Graphene-based nanowire supercapacitors', *Langmuir*, 2014, **30**, (12), pp. 3567–3571
[16] Wang L., Zheng Y., Lu X., *ET AL.*: 'Dendritic copper-cobalt nanostructures/reduced graphene oxide-chitosan modified glassy carbon electrode for glucose sensing', *Sens. Actuators B, Chem.*, 2014, **195**, pp. 1–7
[17] Sun C., Li F., Ma C., *ET AL.*: 'Graphene-Co_3O_4 nanocomposite as an efficient bifunctional catalyst for lithium-air batteries', *J. Mater. Chem. A.*, 2014, **2**, (20), pp. 7188–7196
[18] Tien H.W., Huang Y.L., Yang S.Y., *ET AL.*: 'The production of graphene nanosheets decorated with silver nanoparticles for use in transparent, conductive films', *Carbon*, 2011, **49**, (5), pp. 1550–1560
[19] Yan J.M., Wang Z.L., Wang H.L., *ET AL.*: 'Rapid and energy-efficient synthesis of a graphene–CuCo hybrid as a high performance catalyst', *J. Mater. Chem.*, 2012, **22**, (22), pp. 10990–10993
[20] Moosavifard S.E., Shamsi J., Altafi M.K., *ET AL.*: 'All-solid state, flexible, high-energy integrated hybrid micro-supercapacitors based on 3D LSG/$CoNi_2S_4$ nanosheets', *Chem. Commun.*, 2016, **52**, (89), pp. 13140–13143
[21] Srivastava M., Uddin M. E., Singh J., *ET AL.*: 'Preparation and characterization of self-assembled layer by layer $NiCo_2O_4$-reduced graphene oxide nanocomposite with improved electrocatalytic properties', *J. Alloys Compd.*, 2014, **590**, pp. 266–276
[22] Tahir M., Pan L., Idrees F., *ET AL.*: 'Electrocatalytic oxygen evolution reaction for energy conversion and storage: A comprehensive review', *Nano Energy*, 2017, **37**, pp. 136–157